HHS Public Access

Author manuscript

Cell. Author manuscript; available in PMC 2017 June 30.

Published in final edited form as:

Cell. 2016 June 30; 166(1): 63–76. doi:10.1016/j.cell.2016.05.035.

Mitochondrial Dynamics Controls T Cell Fate Through Metabolic Programming

Michael D. Buck[1,2], **David O'Sullivan**[1], **Ramon I. Klein Geltink**[1], **Jonathan D. Curtis**[1], **Chih-Hao Chang**[2], **David E. Sanin**[1], **Jing Qiu**[1,2], **Oliver Kretz**[3,4], **Daniel Braas**[5], **Gerritje J.W. van der Windt**[6], **Qiongyu Chen**[2], **Stanley Ching-Cheng Huang**[2], **Christina M. O'Neill**[2], **Brian T. Edelson**[2], **Edward J. Pearce**[1,7], **Hiromi Sesaki**[8], **Tobias B. Huber**[3,9], **Angelika S. Rambold**[10,11], and **Erika L. Pearce**[1,*]

[1]Department of Immunometabolism, Max Planck Institute of Immunobiology and Epigenetics, 79108 Freiburg, Germany [2]Department of Pathology and Immunology, Washington University School of Medicine, St. Louis, MO 63110 USA [3]Renal Division, University Medical Center Freiburg, 79106 Freiburg, Germany [4]Department of Neuroanatomy, University of Freiburg, 79104 Freiburg, Germany [5]University of California Los Angeles Metabolomics Center, Los Angeles, CA 90095 USA [6]Academic Medical Center, 1105 AZ Amsterdam, Netherlands [7]Faculty of Biology, University of Freiburg, 79104 Freiburg, Germany [8]Department of Cell Biology, Johns Hopkins University School of Medicine, Baltimore, MD 21205 USA [9]BIOSS Centre for Biological Signaling Studies, 79104 Freiburg, Germany [10]Center for Chronic Immunodeficiency, University Medical Center Freiburg and University of Freiburg, 79106 Freiburg, Germany [11]Department of Developmental Immunology, Max Planck Institute of Immunobiology and Epigenetics, 79108 Freiburg, Germany

SUMMARY

Activated effector T (T_E) cells augment anabolic pathways of metabolism, such as aerobic glycolysis, while memory T (T_M) cells engage catabolic pathways, like fatty acid oxidation (FAO). However, signals that drive these differences remain unclear. Mitochondria are metabolic organelles that actively transform their ultrastructure. Therefore, we questioned whether mitochondrial dynamics controls T cell metabolism. We show that T_E cells have punctate mitochondria, while T_M cells maintain fused networks. The fusion protein Opa1 is required for T_M, but not T_E cells after infection and enforcing fusion in T_E cells imposes T_M cell characteristics and enhances antitumor function. Our data suggest that, by altering cristae morphology, fusion in T_M cells configures electron transport chain (ETC) complex associations

*Correspondence: pearce@ie-freiburg.mpg.de.

AUTHOR CONTRIBUTIONS

M.D.B., D.O., R.I.K.G., D.E.S., D.B., B.T.E., E.J.P., H.S., T.B.H., A.S.R., E.L.P. designed the research and analyzed data. M.D.B., D.O., R.I.K.G., J.D.C., C-H.C., D.E.S., J.Q., O.K., D.B., G.v.d.W., S.C-C.H., and C.M.O. performed experiments. M.D.B. and E.L.P wrote the manuscript.

The authors declare no competing financial interests.

favoring oxidative phosphorylation (OXPHOS) and FAO, while fission in T_E cells leads to cristae expansion, reducing ETC efficiency and promoting aerobic glycolysis. Thus, mitochondrial remodeling is a signaling mechanism that instructs T cell metabolic programming.

Graphical abstract

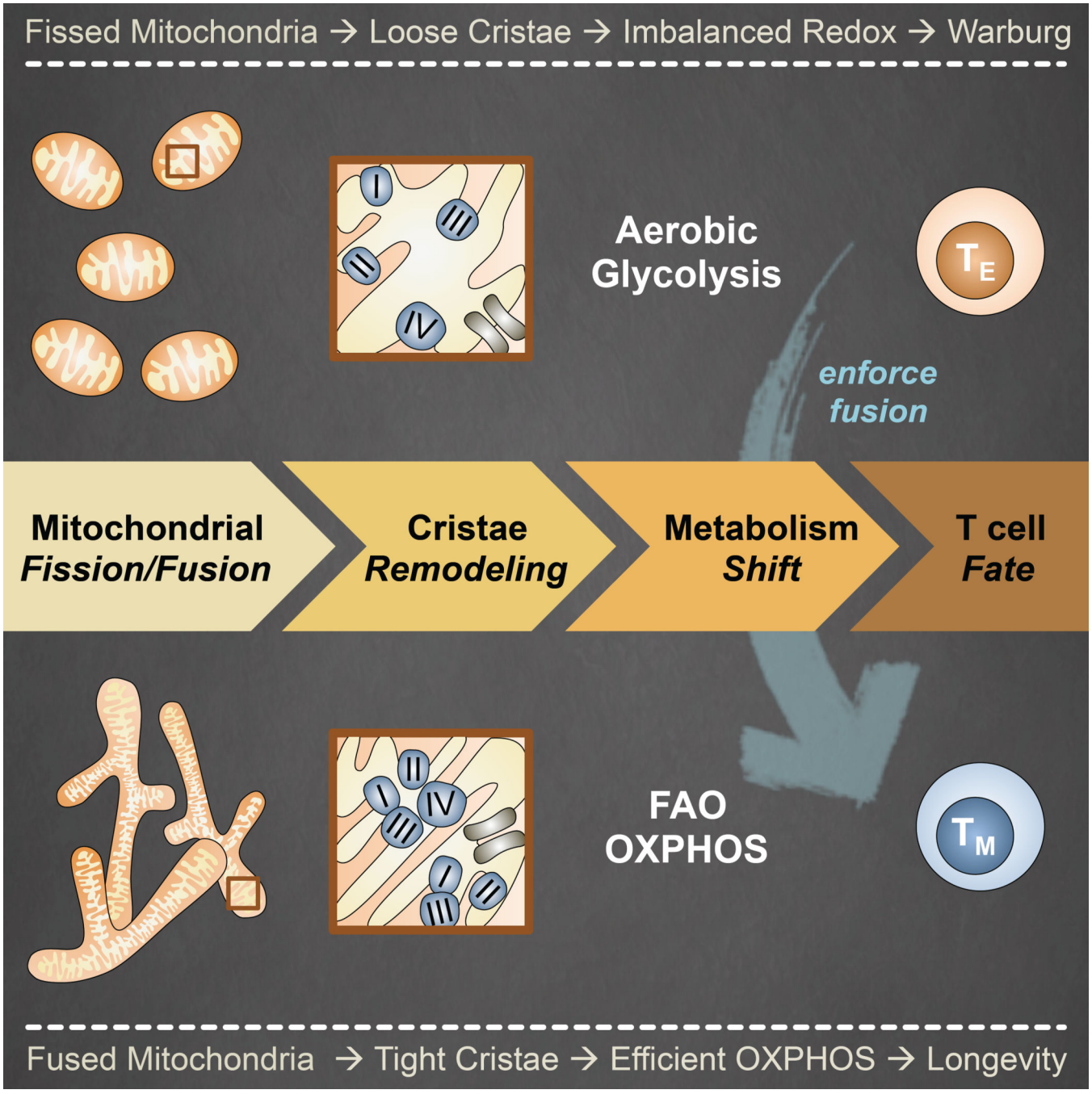

INTRODUCTION

T cells mediate protective immunity against pathogens and cancer and posses the unique ability to proliferate at an unparalleled rate in an adult organism. In this regard, one naïve T (T_N) cell can clonally expand into millions of 'armed' T_E cells in just a few days (Williams and Bevan, 2007). Concomitant with T cell activation is the engagement of aerobic glycolysis and elevated OXPHOS (Chang et al., 2013, Sena et al., 2013), the former of which is characteristic of the Warburg effect shared by tumor cells and unicellular organisms (Vander Heiden et al., 2009). Once antigen is cleared, most T_E cells die, but a subset of long-lived T_M cells persists with enhanced mitochondrial capacity marked by a reliance on FAO to fuel OXPHOS, which equips them to rapidly respond should infection or cancer recur (Pearce et al., 2013). These extensive changes in phenotype and function of T cells go along with a dynamic metabolic range (MacIver et al., 2013, Buck et al., 2015). Failure to engage specific metabolic programs impairs the function and differentiation of T cells. As such, T cells represent an amenable system to study changes in cell metabolism that occur as part of normal development, and not as a result of transformation. Establishing the precise reasons why and how, these and other cells emphasize one particular metabolic pathway over another remains a challenge.

Mitochondria are essential hubs of metabolic activity, antiviral responses, and cell death that constantly remodel their structure via nuclear encoded GTPases (Nunnari and Suomalainen, 2012). Mitochondrial fission generates discrete and fragmented mitochondria that can increase ROS production (Yu et al., 2006), facilitate mitophagy (Frank et al., 2012, Toyama et al., 2016), accelerate cell proliferation (Taguchi et al., 2007), and mediate apoptosis (Youle and Karbowski, 2005). Dynamin-related protein 1 (Drp1) is a cytosolic protein that translocates to the outer mitochondrial membrane (OMM) upon phosphorylation to scission mitochondria. Fusion of mitochondria into linear or tubular networks limits deleterious mutations in mitochondrial DNA (mtDNA) (Santel et al., 2003), induces supercomplexes of the ETC maximizing OXPHOS activity (Cogliati et al., 2013, Mishra et al., 2014), and enhances endoplasmic reticulum (ER) interactions important for Ca^{2+} flux (de Brito and Scorrano, 2008). In addition, mitochondria elongate as a survival mechanism in response to nutrient starvation and stress, linking fusion to cell longevity (Gomes et al., 2011, Rambold et al., 2011, Friedman and Nunnari, 2014). OMM fusion is mediated by mitofusin 1 and 2 (Mfn1, Mfn2), while inner membrane fusion is controlled by optic atrophy 1 (Opa1). Total deletion in any of these proteins is embryonically lethal and mutations in the genes that encode them underlie the cause of several human diseases (Chan, 2012, Archer, 2014).

Mitochondrial membrane remodeling is acutely responsive to changes in cell metabolism (Mishra and Chan, 2016, Wai and Langer, 2016), but whether it instructs metabolic pathway utilization has been inferred but not extensively studied. In general, deletion of any of the dynamics machinery perturbs OXPHOS and glycolytic rates at baseline (Liesa and Shirihai, 2013). Tissue-specific deletion of Mfn2 in muscles of mice disrupts glucose homeostasis (Sebastian et al., 2012) and Drp1 ablation in the liver results in reduced adiposity and elevated whole-body energy expenditure, protecting mice from diet-induced obesity (Wang et al., 2015). A recent study has also suggested a link between Drp1 mediated fission and its affect on glycolysis during cell transformation (Serasinghe et al., 2015). The central question

of whether fission/fusion and associated changes in cristae morphology actively control the adoption of distinct metabolic programs and therefore regulates T cell responses however, remains unanswered.

RESULTS

Unlike T_E cells, T_M cells maintain a fused mitochondrial network

We reported that T_M cells have more mitochondrial mass than T_E or T_N cells and suggested that mitochondria in these T cell subsets are morphologically distinct (van der Windt et al., 2012, van der Windt et al., 2013). These observations prompted us to assess mitochondrial structure in T cells. We infected mice with *Listeria monocytogenes* expressing ovalbumin (OVA) (LmOVA) and isolated T_E and T_M cells for ultrastructure analysis by electron microscopy (EM). We found that T_E cells had small, distinct mitochondria dispersed in the cytoplasm, while T_M cells had densely packed, somewhat tubular, mitochondria (Figure 1A). To investigate these morphological differences, we differentially cultured activated OVA-specific T cell receptor (TCR) transgenic OT-I cells in interleukin-2 (IL-2) and IL-15 to generate IL-2 T_E and IL-15 T_M cells (Figure S1) (Carrio et al., 2004). These culture conditions approximate T cell responses *in vivo* and allow us to generate large numbers of cells amenable to further experimentation *in vitro* (O'Sullivan et al., 2014). We found that IL-2 T_E and IL-15 T_M cells possessed similar mitochondrial ultrastructure as their *ex vivo* isolated counterparts (Figure 1B). Using confocal microscopy we observed that while a day after activation the mitochondria appeared fused, from days 2–6 the IL-2 T_E cells exhibited predominantly punctate mitochondria (Figure 1C). In contrast, once cells were exposed to IL-15, a cytokine that supports T_M cell formation (Schluns et al., 2002), the mitochondria formed elongated tubules. Magnified images from these experiments emphasized the marked differences in mitochondrial morphology between IL-2 T_E and IL-15 T_M cells (Figure 1D). We also examined the protein expression of several critical regulators of mitochondrial dynamics. We found that by day 6, fusion mediators Mfn2 and Opa1 were lower in T_E cells compared to T_M cells, while fission factor Drp1 was phosphorylated at its activating site Ser616 in T_E cells (Figure 1E) (Marsboom et al., 2012). Together these data suggest that mitochondria in T_E cells are actively undergoing fission while in T_M cells, these organelles exist in a fused state.

Mitochondrial inner membrane fusion protein Opa1 is necessary for T_M cell generation

To test whether mitochondrial fusion was important for T_M cell development we crossed Mfn1, Mfn2, and Opa1 floxed mice to OT-I CD4 Cre transgenic mice to conditionally delete these proteins in T cells. Peripheral T cell frequencies in these mice were grossly normal (**data not shown**). We differentially cultured $Mfn1^{-/-}$, $Mfn2^{-/-}$, and $Opa1^{-/-}$ OT-I T cells in IL-2 and IL-15 and found that only $Opa1^{-/-}$ T cells had a survival defect when cultured in IL-15 (Figure 2A), but not in IL-2. We measured the efficiency of gene deletion by mRNA and/or protein analyses (Figure S2A–C). While Mfn1 and 2 were efficiently deleted, we found residual expression of Opa1 particularly in IL-15 T_M cells, suggesting that cells that retained some expression of Opa1 in IL-15 cultures had a survival advantage (Figure 2A). Assessment of mitochondrial ultrastructure revealed that the cristae were altered and disorganized in the absence of Opa1 in agreement with published results for other cells

(Figure 2B) (Zhang et al., 2011, Cogliati et al., 2013). Consistent with their survival defect, Opa1$^{-/-}$ IL-15 T_M cells had decreased OXPHOS activity, as measured by O_2 consumption rate (OCR, an indicator of OXPHOS) to extracellular acidification rate (ECAR, an indicator of aerobic glycolysis) ratio, and spare respiratory capacity (SRC), compared to normal cells (Figure 2C). SRC is the extra mitochondrial capacity available in a cell to produce energy under conditions of increased work or stress and is thought to be important for long-term cell survival and function (measured as OXPHOS activity above basal after uncoupling with FCCP) (Nicholls, 2009, van der Windt et al., 2012). To determine whether Opa1 is required for T_M cell development *in vivo*, we adoptively transferred Opa1$^{-/-}$ OT-I T_N cells into congenic recipients, infected these mice with LmOVA, and assessed T_M cell formation in the weeks after infection. Control and Opa1$^{-/-}$ OT-I T cells mounted normal T_E cell responses (day 7) to infection, while Opa1$^{-/-}$ OT-I T_M cell formation (days 14–21) was drastically impaired (Figure 2D). Consistent with diminished T_M cell development, a significantly higher proportion of short-lived effector to memory precursor effector cells were present within the Opa1$^{-/-}$ OT-I donor cell population 7 days after infection (Figure S2D) (Kaech et al., 2003). In addition, at day 10 post infection, a time point when T_E cells contract while T_M cells emerge, Opa1$^{-/-}$ T cells isolated *ex vivo* had decreased SRC compared to control cells (Figure S2E), correlating with their decreased survival. To assess whether Opa1$^{-/-}$ T_M cells existed in too low an abundance to be discerned by flow cytometry, we challenged these mice with a second infection. We observed no recall response (day 3 and 6 p.c.) from Opa1$^{-/-}$ T cells when assessing frequency (Figure 2E) or absolute numbers (Figure 2F), while there was considerable expansion of control donor cells. These data illustrate that Opa1 is required for T_M, but not T_E cell generation.

Mitochondrial fusion imposes a T_M cell phenotype, even in the presence of activating signals

Genetic loss of function of Opa1 revealed that this protein is critical for T_M cell formation. Given the fused phenotype of mitochondria in T_M cells, we hypothesized that Opa1-mediated mitochondrial fusion supports the metabolism needed for T_M cell development. We used a gain of function approach to enhance mitochondrial fusion. Culturing T cells with the ‘fusion promoter’ M1 (Wang et al., 2012), and the ‘fission inhibitor’ Mdivi-1 (Cassidy-Stone et al., 2008) (Figure 3A) induced mitochondrial fusion in IL-2 T_E cells, rendering them morphologically similar to IL-15 T_M cells (Figure 3B). Treatment with these drugs enhanced other T_M cell properties in activated IL-2 T_E cells, including increased mitochondrial mass (Figure 3C), OXPHOS and SRC (Figure 3D), CD62L expression (Figure 3E) and robust metabolic activity, as indicated by bioenergetic profiling in response to secondary stimulation with PMA+ionomycin, followed by addition of oligomycin (ATP synthase inhibitor), FCCP, and rotenone with antimycin A (ETC complex I and III inhibitors), all drugs that stress the mitochondria (Figure 3F and S3A). However, we did not observe increased mtDNA in these cells (Figure S3B). We found that ECAR and the OCR/ECAR ratio increased after drug treatment (Figure S3C), indicating elevated metabolic activity overall, with a predominant increase in OXPHOS over glycolysis. While we observed these changes in mitochondrial activity, we did not measure any significant differences in mitochondrial membrane potential or ROS after drug treatment (Figure S3D). The expression of other activation markers were also not substantially affected, although a

small decrease in KLRG1 and increase in CD25 was measured (Figure S3E). Additionally, we performed a genetic gain of function experiment and transduced activated IL-2 T_E cells with retrovirus expressing Mfn1, Mfn2, or Opa1. Similar to enforcement of fusion pharmacologically, we found that cells transduced with Opa1 had more mitochondria (Figure 3G) and OXPHOS (Figure 3H), than empty vector control or Mfn-transduced T cells, as well as increased overall metabolic activity, with a predominant increase in OXPHOS over glycolysis (Figure S3F). T_M cell associated markers such as CCR7 and CD127 were increased on transduced cells, as well as T_E cell proteins, such as PD-1 (Figure S3G). Overexpression of each target gene over the control was confirmed by mRNA expression (Figure S3H). Together our results show that mitochondrial fusion confers T_M cell phenotypes on activated T_E cells even in culture conditions that program T_E cell differentiation.

T cell mitochondrial fusion improves adoptive cellular immunotherapy against tumors

A consideration when designing adoptive cellular immunotherapy (ACI) is to improve T cell fitness during *ex vivo* culture so that when T cells are re-introduced into a patient they are able to function efficiently and persist over time (Restifo et al., 2012, Maus et al., 2014, O'Sullivan and Pearce, 2015). Our data showed that fusion-promoting drugs created metabolically fit T cells. We predicted that enforcing fusion would also enhance the longevity of IL-2 T_E cells *in vivo*. To test this, we adoptively transferred control and M1+Mdivi-1 treated OT-I T cells into congenic mice and tracked donor cell survival. We found significantly more drug treated T cells in the spleen (Figure 3I) and lymph nodes (Figure 3J) 2 days after transfer. To determine if the persistence of these cells would be maintained better long term than controls, we infected mice with LmOVA >3 weeks later and measured T cell responses against the bacteria. We found that drug-treated cells selectively expanded in response to infection (Figure 3K) and could be recovered in significantly greater numbers in the spleen 6 days post challenge (Figure 3L).

Next, we assessed whether these drugs could be used to promote T cell function in an ACI model. We injected EL4-OVA tumor cells into mice. Then either 5 or 12 days later we adoptively transferred IL-2 T_E cells that had been treated with DMSO or M1+Mdivi-1. In both settings, mice that received 'fusion-promoted' T cells were able to control tumor growth significantly better than mice that received control treated cells (Figure 4A and B). The cytolytic ability (Figure S4A) and proliferation (Figure S4B) of the fusion enforced IL-2 T_E cells were similar to controls, however, they expressed significantly higher levels of IFN-γ and TNF-α when restimulated with PMA+ionomycin *in vitro* (Figure S4C). We also exposed activated human T cells to M1+Mdivi-1 treatment *in vitro* and found that they had visibly more fused mitochondria (Figure 4C), and exhibited the bioenergetic profile (Figure 4D) and surface marker expression (Figure 4E) characteristic of T_M cells, compared to control treated cells. Parameters such as mitochondrial mass (Figure 4E) and other surface markers (Figure S4D) were not significantly altered. These data suggest that promoting fusion in T cells may be a translatable treatment for enhancing human therapy.

Mitochondrial fusion promotes T_M cell metabolism, but Opa1 is not required for FAO

Our data showed that Opa1 was necessary for T_M cell formation, but the question of how Opa1 acted to support T_M cells remained. We hypothesized that mitochondrial fusion, via Opa1 function, was needed for FAO, as the engagement of this pathway is required for T_M cell development and survival (Pearce et al., 2009, van der Windt et al., 2012, van der Windt et al., 2013). This hypothesis was based on our observations that these two processes seemed to be linked in T_M cells and also on a recent report that mitochondrial fusion is important for efficient FAO via lipid droplet trafficking under starvation conditions (Rambold et al., 2015). We treated IL-2 T_E and IL-15 T_M cells with M1+Mdivi-1 or vehicle and then measured OCR in response to etomoxir, a specific inhibitor of mitochondrial long chain FAO (Deberardinis et al., 2006), and mitochondrial inhibitors. We found that the increased OCR and SRC evident in these cells after M1+Mdivi-1 treatment was due to enhanced FAO (Figure 5A and S5A). IL-2 T_E cells transduced with Opa1 also exhibited elevated OCR that decreased in the presence of etomoxir compared to controls (Figure 5B). Bone marrow derived macrophages (BM-Macs) cultured with M1+Mdivi-1 increased OCR and SRC to levels similar to M2 polarized macrophages, which engage FAO much like T_M cells do (Figure S5B) (Huang et al., 2014). Importantly, M1+Mdivi-1 treatment did not increase OCR (Figure 5C) or affect ECAR (Figure S5C) in $Opa1^{-/-}$ IL-2 T_E cells compared to controls, suggesting a requirement for Opa1 in augmenting OCR and FAO. However, in contrast to what we expected, when we assessed bioenergetics of $Opa1^{+/+}$ and $Opa1^{-/-}$ IL-2 T_E (Figure 5D) and *ex vivo* isolated T_E cells (Figure 5E), we found that both are equally responsive to etomoxir. Our results show that while Opa1 can promote FAO in T cells, it is not compulsory for engagement of this metabolic pathway.

Mitochondrial cristae remodeling signals metabolic adaptations in T_M and T_E cells

Although $Opa1^{+/+}$ and $Opa1^{-/-}$ IL-2 T_E cells could equally engage FAO (Figure 5D), we observed that ECAR was significantly increased in $Opa1^{-/-}$ cells both *in vitro* and *ex vivo* (Figure 6A). Furthermore, unlike controls, we observed no additional drop of OCR in $Opa1^{-/-}$ IL-2 T_E cells after the addition of oligomycin (Figure 6B), suggesting that in the absence of Opa1, only FAO supports OXPHOS, and that substrates, such as glucose-derived pyruvate, are not used for mitochondrial ATP production in this setting. We cultured $Opa1^{+/+}$ and $Opa1^{-/-}$ IL-2 T_E cells with ^{13}C-labeled glucose and traced ^{13}C into TCA cycle metabolites. While the percent of ^{13}C-labeled pyruvate was higher in $Opa1^{-/-}$ T cells, the frequency of ^{13}C-labeled TCA cycle intermediates was significantly reduced in $Opa1^{-/-}$ T cells compared to controls (Figure 6C and S6A), a result that is supported by their higher ECAR (Figure 6A). These data suggested that without mitochondrial fusion, pyruvate is preferentially secreted as lactate, rather than oxidized in the mitochondria. Therefore, we questioned whether FAO is a ‘default’ pathway for mitochondria in a resting, or fused state (i.e. Opa1 sufficiency), and that the induction of aerobic glycolysis is a major downstream effect of fission (i.e. Opa1 deficiency). If this were the case, then a balance between fission and fusion, modulated by proteins such as Opa1, could act as a primary signal to dictate the metabolic phenotype of T cells. In support of this idea, T cells from polyclonal T cell-conditional deleted Opa1 mice had higher ECAR and an increased proportion of CD8 T cells with an activated effector phenotype in the basal state based on surface marker expression (Figure S6B).

Opa1 is critical for inner mitochondrial membrane fusion, but also for other processes like cristae remodeling (Frezza et al., 2006, Cogliati et al., 2013). We observed major changes in cristae morphology in Opa1$^{-/-}$ T cells (Figure 2B). Given the importance of Opa1 in T_M cell development (Figure 2), we further assessed cristae morphology in T_E and T_M cells isolated *ex vivo* after LmOVA infection (Figure 6D), as well as IL-2 T_E and IL-15 T_M cells (Figure 6E), and found that T_E cells had many cristae with slightly wider and loosely organized intermembrane space, than T_M cells. Opa1 overexpression induces cristae tightening and close association of ETC complexes in the inner mitochondrial membrane (Cogliati et al., 2013, Civiletto et al., 2015). Therefore, we surmised that in the absence of Opa1, cristae disorganization leads to dissociation of ETC complexes and subsequently less efficient ETC activity in T cells (Figure 2C). We assessed OCR after oligomycin in relation to OCR after rotenone and antimycin A treatment (i.e. proton leak), which indicates the coupling efficiency of OXPHOS to mitochondrial ATP production. Consistent with decreased OXPHOS efficiency, we observed elevated proton leak in Opa1$^{-/-}$ T cells compared to controls (Figure 6F). This was also true for *ex vivo* isolated T_E cells compared to T_M cells (Figure 6G), as well as IL-2 T_E and IL-15 T_M cells (Figure 6H). Together these data suggest that there are cristae differences between T_E and T_M cells, which may contribute to their distinct metabolic phenotypes.

We reasoned that fusion renders tightly configured cristae, which results in closely associated ETC complexes and efficient OXPHOS (Patten et al., 2014), producing conditions that favor the entrance of pyruvate into the TCA cycle. NADH generated from the TCA cycle is able to easily donate electrons to complex I, which are passed efficiently along the ETC. Our data suggest that this predominantly occurs in T_M cells. However, if electron transport across the ETC became less efficient, caused by physical separation of the individual complexes due to cristae remodeling via mitochondrial fission, then electrons could linger in the complexes and imbalance redox reactions. NADH levels would build, slowing forward momentum of the TCA cycle. To restore redox balance, cells could augment glycolysis and shunt pyruvate as excreted lactate (i.e. aerobic glycolysis), regenerating NAD^+ from cytosolic NADH. We speculate that this occurs in T_E cells. Correlating with this idea, we previously reported that T_E and T_M cells have different ratios of NAD^+/NADH (i.e. redox balance) with T_M cells maintaining higher NAD^+/NADH than T_E cells. We also showed that NADH levels dramatically rise in T_M cells compared to T_E cells when exposed to rotenone and antimycin A, indicating that T_M cells consume more NADH for the purpose of donating electrons to the ETC (van der Windt et al., 2012). Together our data suggest that fission and fusion regulate cristae remodeling, which alter ETC efficiency and redox balance, ultimately controlling metabolic adaptations in T cells.

To examine this idea further, we assessed cristae morphology in T_E and T_M cells by EM after TCR stimulation. We hypothesized that if cristae remodeling induces aerobic glycolysis, changes in cristae structure could be visualized after T cell activation. T_M cells rapidly augment aerobic glycolysis when restimulated (van der Windt et al., 2013). We activated IL-15 T_M cells with αCD3/CD28 beads (Figure 6I), or with PMA+ionomycin (Figure S6C), in the presence or absence of Mdivi-1 to modulate activity of mitochondrial fission protein Drp1 (Cassidy-Stone et al., 2008). We observed dramatic changes to cristae morphology by EM, with the intermembrane space widening over time in controls compared

to drug treated cells. These data are consistent with the hypothesis that fission-induced mitochondrial cristae remodeling supports metabolic reprogramming in T cells.

T_M cells maintain tight cristae with closely associated ETC complexes

Our data suggested that unlike T_E cells, T_M cells have tight cristae with closely associated ETC complexes. To investigate this biochemically, we treated native lysates of IL-2 T_E and IL-15 T_M cells with increasing concentrations of digitonin to disrupt cell membranes (including mitochondrial). The crude membrane-bound fraction was separated from solubilized proteins by centrifugation. Both pellet and soluble supernatants were loaded on a denaturing reducing gel and then probed for various mitochondrial proteins by western blot. We found that mitochondria in IL-2 T_E cells were susceptible to digitonin disruption, indicated by the fact that ETC complex proteins became less detectable in the pellet, and enriched in the soluble fraction in 0.5% detergent (Figure 6J and S6D). This was in contrast to IL-15 T_M cells, where ETC proteins did not solubilize to the same extent as those in IL-2 T_E cells into the supernatant, even when 2% digitonin was used. To investigate whether this phenomenon was unique to the mitochondrial compartment, we also probed for the ER integral protein calnexin and found that it solubilized similarly in 0.5% digitonin in both cell types. Overall these data suggest that there is more exposed mitochondrial membrane between proteins in IL-2 T_E than IL-15 T_M cells, and is consistent with the idea that T_M cells have tight cristae which yield efficient ETC activity, while T_E cells have looser cristae with less efficient ETC activity, ultimately supporting their distinct metabolic phenotypes.

Mitochondrial fission in activated immune cells facilitates aerobic glycolysis

Our data supports a model wherein cristae remodeling, through fission and fusion events, is a mechanism to regulate efficient OXPHOS and FAO in T_M cells, as well as the induction of aerobic glycolysis in T_E cells. To more directly test this idea, we assessed ECAR of IL-15 T_M cells stimulated with αCD3/28 beads in the presence or absence of Mdivi-1. We found that when mitochondrial fission protein Drp1 was inhibited with Mdivi-1, T cell activation did not robustly increase aerobic glycolysis when compared to controls (Figure 6K), which correlated with our EM data (Figure 6I). Since fission is associated with cell division (Taguchi et al., 2007), we tested our idea in a non-proliferating cell that substantially augments aerobic glycolysis upon stimulation (Krawczyk et al., 2010). We stimulated bone marrow derived dendritic cells (BM-DCs) and macrophages (BM-Macs) with lipopolysaccharide (LPS) with or without interferon (IFN)-γ in the presence or absence of Mdivi-1 and measured ECAR. Aerobic glycolysis was curtailed in BM-DCs and BM-Macs after stimulation when Drp1 was inhibited (Figure 6L). The blunted ECAR in Mdivi-1 treated cells correlated with decreased nitric oxide synthase 2 (Nos2) protein expression in the BM-Macs (Figure 6M), indicating that their activation was also repressed. These data show that cristae remodeling and/or fission acts as a signal to drive the induction of aerobic glycolysis, and subsequent cell activation via Drp1.

DISCUSSION

Although T_M cells rely on FAO for development and survival, precisely why T_M cells utilize FAO and the signals that drive the induction of aerobic glycolysis in T_E cells remain unclear.

Our data suggest that manipulating the structure of a single organelle can have profound consequences that impact metabolism and ultimately cell differentiation. We found that Opa1 regulated tight cristae organization in T_M cells, which facilitated efficient ETC activity and favorable redox balance, allowing continued entrance of pyruvate into mitochondria. We originally hypothesized that Opa1 would be required for FAO. However, we found that Opa1$^{-/-}$ IL-2 T_E and *ex vivo* T_E cells generated during infection utilized FAO to the same level as controls. While this was true for T_E cells, this may not be the case for T_M cells, whose survival is severely impaired *in vitro* and *in vivo* when Opa1 deficient. It is possible that Opa1$^{-/-}$ T cells are unable to form T_M cells because they cannot efficiently engage FAO under the metabolic constraints imposed during T_M cell development. Previous studies point to the existence of a 'futile' cycle of fatty acid synthesis (FAS) and FAO in T_M cells (O'Sullivan et al., 2014, Cui et al., 2015) whereby carbon derived from glucose is used to build fat that is subsequently burned by mitochondria. T_M cells have a lower overall metabolic rate than T_E cells, and tightly configured cristae may be important to ensure that any pyruvate generated will efficiently feed into the TCA cycle not only for reducing equivalents, but also for deriving citrate for FAS. Without tight cristae and efficient ETC activity, electrons may loiter in the complexes causing more ROS which could be damaging, but also provide signals that drive cell activation (Sena et al., 2013).

We did not observe a defect in T_M cell survival in Mfn1$^{-/-}$ or Mfn2$^{-/-}$ T cells, but this does not exclude the possibility that OMM fusion or additional activities ascribed to each protein are not important. Mfn1 and Mfn2 form homotypic and heterotypic interactions, suggesting that in the absence of one, the other can compensate (Chen et al., 2003). Our results show that unlike Opa1$^{-/-}$ T cells, *in vitro* cultured Mfn1$^{-/-}$ or Mfn2$^{-/-}$ T cells do not have a survival defect when differentiated in IL-15, even though, like Opa1$^{-/-}$ T cells, they are more glycolytic and OXPHOS-impaired compared to controls (**data not shown**). Our imaging data showed that T_M cells maintained fused mitochondrial networks, suggesting that OMM fusion also has a compulsory role in T_M cell development. However, unlike Opa1, retroviral expression of Mfn1 and Mfn2 did not confer a T_M cell phenotype in T_E cells. In this setting, an increase in OMM fusion without a concomitant increase in inner membrane fusion may still yield loose cristae morphology and a redox state that by default results in sustained excretion of lactate.

The question of what initial signals drive T cell mitochondrial remodeling still remains. In the case of T_M cell development, withdrawal of activating signals and growth factors may induce fusion, consistent with previous reports that starvation induces mitochondrial hyperfusion (Rambold et al., 2015), an effect we also observe in T_E cells after IL-2 withdrawal (**data not shown**). However, pro-survival signals from cytokines like IL-15 or IL-7 are needed to sustain T_M cell viability and metabolically remodel these cells for FAS and FAO via increased CPT1a (van der Windt et al., 2012) and aquaporin 9 expression (Cui et al., 2015). Factors such as these may enforce fusion and would be consistent with our observations that mitochondria in activated T cells subsequently cultured in IL-15 fuse over time. Another possibility is that during metabolic stress, Opa1 is activated via sirtuin 3 (SIRT3) (Samant et al., 2014). Sirtuins are post-translational modifiers that are activated by NAD^+, directly tying their activity to cell metabolism (Houtkooper et al., 2012, Wang and

Green, 2012). We previously published that there is more available NAD^+ in T_M cells (van der Windt et al., 2012), which may correlate with this scenario.

In T_E cells a day after TCR stimulation, we saw activation of Drp1 via its phosphorylation site Ser616 prior to seeing a fissed phenotype. TCR signals instigate Ca^{2+} flux that promotes the phosphatase activity of calcineurin (Smith-Garvin et al., 2009), which in turn dephosphorylates Drp1 at Ser637, leading to its activation (Cereghetti et al., 2008). Initial Drp1 activation could facilitate some level of fission and cristae remodeling, tipping off aerobic glycolysis via the initial shunting of pyruvate to lactate. Although inhibition of Drp1 blocks activation induced ECAR, our preliminary data do not show overt mitochondrial fragmentation in the early hours after TLR stimulation of DC or macrophages (**data not shown**). This however, does not exclude the possibility that Drp1 is mediating subtle changes to mitochondrial structure that are not discernable by confocal microscopy. Drp1 also affects cristae structure by altering the fluidity of the mitochondrial membrane (Benard et al., 2007). While Drp1 has been implicated in mitochondrial positioning at the immune synapse (Baixauli et al., 2011), lymphocyte chemotaxis (Campello et al., 2006), and ROS production during T cell activation (Roth et al., 2014), our data suggest that in addition to these processes, cristae remodeling via fission underlies the programming of cells to aerobic glycolysis.

We show that mitochondria in IL-2 T_E cells are more susceptible to digitonin disruption than IL-15 T_M cells, suggesting a more exposed membrane with less densely packed protein complexes. This relatively enhanced permeability however, does not mean that their mitochondria are damaged, or unable to function. In fact, although T_E cells have less efficient OXPHOS in terms of coupling to ATP synthesis, T_E cells are very metabolically active with high OCR and ECAR (Chang et al., 2013, Sena et al., 2013). Our experiments involving pharmacological enforcement of mitochondrial fusion promoted OCR and SRC (and ECAR, albeit to a lesser extent) in IL-2 T_E cells. The drug modified cells maintained full T_E cell function with no effect on cytolytic ability or proliferation, but possessed enhanced cytokine expression. Fusion and/or cristae tightening boosted oxidative capacity in T_E cells, endowing them with longevity and persistence, while their higher aerobic glycolysis supported increased cytokine production, which may explain their superior antitumor function.

Our data suggest a model where morphological changes in mitochondria are a primary signal that shapes metabolic reprogramming during cellular quiescence or activation. We speculate that fission associated expansion of cristae as a result of TCR stimulation physically separates ETC complexes, decreasing ETC efficiency. With delayed movement of electrons down the ETC, NADH levels rise, slowing forward momentum of the TCA cycle and cause an initial drop in ATP. To correct redox balance, cells will export pyruvate to lactate to regenerate NAD^+ in the cytosol, which can enter the mitochondria through various shuttles to restore redox balance (Dawson, 1979) and increase flux through glycolysis to restore ATP levels, all contributing to the Warburg effect in activated T cells. When cristae are tightly configured, the ETC works efficiently and maintains entrance of pyruvate into the mitochondria with a favorable redox balance. In this case, cristae morphology as a result of fusion directs T_M cell formation and retains these cells in a quiescent state. Thus,

mitochondrial dynamics controls the balance between metabolic pathway engagement and T cell fate.

EXPERIMENTAL PROCEDURES

See the Supplemental Information for details

Mice and immunizations

Mice were purchased from The Jackson Laboratory. LmOVA deleted for *actA* was used for primary and secondary immunizations. For tumor studies, EL4 lymphoma cells expressing OVA (EL4-OVA) were injected subcutaneously (s.c.) into the flank of mice.

Flow cytometry and imaging

Antibody and H2-$K^bOVA_{257–264}$ (K^bOVA) MHC-peptide tetramer staining were performed as described (Chang et al., 2015). For EM, cells were fixed in 2% paraformaldehyde, 2.5% glutaraldehyde in 100 mM sodium cocodylate containing 0.05% malachite green.

Metabolism assays

OCR and ECAR were measured using a 96 well XF or XFe Extracellular Flux Analyzer (EFA) (Seahorse Bioscience). For fission inhibition studies, cells were plated in assay media with 10 μM Mdivi-1 or vehicle control (DMSO) followed by assay media or αCD3/CD28 bead or 20 ng/mL LPS ± 50 ng/mL IFN-γ injection.

Glucose tracing

Cells were activated in glucose free media (prepped with dialyzed FBS) supplemented with 11 mM glucose. After 3 days, cells were washed and cultured overnight in media replaced with 11 mM D-[1,2^{13}C] glucose. Metabolites were extracted with MeOH and analyzed by MS.

Adoptive transfers

For *in vivo* T_M cell studies, ≤10^4 OT-I^+ $CD8^+$ donor cells/mouse were transferred intravenously (i.v.) into congenic C57BL/6 mice. For *in vivo* survival experiments, 1–2×10^6 day 6 IL-2 T_E treated cells/mouse were injected i.v. into congenic C57BL/6 mice. For tumor studies, 1–5×10^6 day 6 IL-2 T_E treated cells/mouse were injected i.v. into previously EL4-OVA inoculated mice.

Retroviral transduction

Activated OT-I splenocytes were transduced with control (empty vector) or Mfn1, Mfn2, Opa1 expressing retrovirus by centrifugation. GFP or human CD8 marked retroviral expression.

Statistical analysis

Comparisons for two groups were calculated using unpaired two-tailed student's *t*-tests and one-way ANOVA followed by Bonferroni's multiple comparison tests for more than two

groups. Comparisons over time were calculated using two-way ANOVA followed by Bonferroni's multiple comparison tests.

Supplementary Material

Refer to Web version on PubMed Central for supplementary material.

Acknowledgments

We thank David Chan (Caltech) for Mfn1/2 floxed mice, Tom Graeber (DMMP, David Geffen School of Medicine, UCLA Metabolomics Center), Wandy Beatty (Molecular Microbiology Imaging Facility, Washington University School of Medicine), Erica Lantelme, Dorjan Brinja, Barbara Joch, Hani Suleiman, Elena Tonc, Tara Bradstreet, and Elizabeth Schwarzkopf for technical assistance.

This work was funded by the NIH (CA181125 and AI091965 to E.L.P. and AI110481 to E.J.P.), the Burroughs Wellcome Fund (Investigator in the Pathogenesis of Infectious Disease Award to E.L.P. and Career Award for Medical Scientists to B.T.E.), the BMBF (A.S.R.), the Max Planck Society, and the NSF Graduate Research Fellowship DGE-1143954 (M.D.B.).

REFERENCES

Archer SL. Mitochondrial fission and fusion in human diseases. N Engl J Med. 2014; 370:1074. [PubMed: 24620884]

Baixauli F, Martin-Cofreces NB, Morlino G, Carrasco YR, Calabia-Linares C, Veiga E, Serrador JM, Sanchez-Madrid F. The mitochondrial fission factor dynamin-related protein 1 modulates T-cell receptor signalling at the immune synapse. EMBO J. 2011; 30:1238–1250. [PubMed: 21326213]

Benard G, Bellance N, James D, Parrone P, Fernandez H, Letellier T, Rossignol R. Mitochondrial bioenergetics and structural network organization. J Cell Sci. 2007; 120:838–848. [PubMed: 17298981]

Buck MD, O'Sullivan D, Pearce EL. T cell metabolism drives immunity. J Exp Med. 2015; 212:1345–1360. [PubMed: 26261266]

Campello S, Lacalle RA, Bettella M, Manes S, Scorrano L, Viola A. Orchestration of lymphocyte chemotaxis by mitochondrial dynamics. J Exp Med. 2006; 203:2879–2886. [PubMed: 17145957]

Carrio R, Bathe OF, Malek TR. Initial antigen encounter programs CD8+ T cells competent to develop into memory cells that are activated in an antigen-free, IL-7- and IL-15-rich environment. J Immunol. 2004; 172:7315–7323. [PubMed: 15187107]

Cassidy-Stone A, Chipuk JE, Ingerman E, Song C, Yoo C, Kuwana T, Kurth MJ, Shaw JT, Hinshaw JE, Green DR, Nunnari J. Chemical inhibition of the mitochondrial division dynamin reveals its role in Bax/Bak-dependent mitochondrial outer membrane permeabilization. Dev Cell. 2008; 14:193–204. [PubMed: 18267088]

Cereghetti GM, Stangherlin A, Martins de Brito O, Chang CR, Blackstone C, Bernardi P, Scorrano L. Dephosphorylation by calcineurin regulates translocation of Drp1 to mitochondria. Proc Natl Acad Sci U S A. 2008; 105:15803–15808. [PubMed: 18838687]

Chan DC. Fusion and fission: interlinked processes critical for mitochondrial health. Annu Rev Genet. 2012; 46:265–287. [PubMed: 22934639]

Chang CH, Curtis JD, Maggi LB Jr, Faubert B, Villarino AV, O'Sullivan D, Huang SC, van der Windt GJ, Blagih J, Qiu J, Weber JD, Pearce EJ, Jones RG, Pearce EL. Posttranscriptional control of T cell effector function by aerobic glycolysis. Cell. 2013; 153:1239–1251. [PubMed: 23746840]

Chang CH, Qiu J, O'Sullivan D, Buck MD, Noguchi T, Curtis JD, Chen Q, Gindin M, Gubin MM, van der Windt GJ, Tonc E, Schreiber RD, Pearce EJ, Pearce EL. Metabolic Competition in the Tumor Microenvironment Is a Driver of Cancer Progression. Cell. 2015; 162:1229–1241. [PubMed: 26321679]

Chen H, Detmer SA, Ewald AJ, Griffin EE, Fraser SE, Chan DC. Mitofusins Mfn1 and Mfn2 coordinately regulate mitochondrial fusion and are essential for embryonic development. J Cell Biol. 2003; 160:189–200. [PubMed: 12527753]

Civiletto G, Varanita T, Cerutti R, Gorletta T, Barbaro S, Marchet S, Lamperti C, Viscomi C, Scorrano L, Zeviani M. Opa1 overexpression ameliorates the phenotype of two mitochondrial disease mouse models. Cell Metab. 2015; 21:845–854. [PubMed: 26039449]

Cogliati S, Frezza C, Soriano ME, Varanita T, Quintana-Cabrera R, Corrado M, Cipolat S, Costa V, Casarin A, Gomes LC, Perales-Clemente E, Salviati L, Fernandez-Silva P, Enriquez JA, Scorrano L. Mitochondrial cristae shape determines respiratory chain supercomplexes assembly and respiratory efficiency. Cell. 2013; 155:160–171. [PubMed: 24055366]

Cui G, Staron MM, Gray SM, Ho PC, Amezquita RA, Wu J, Kaech SM. IL-7-Induced Glycerol Transport and TAG Synthesis Promotes Memory CD8+ T Cell Longevity. Cell. 2015; 161:750–761. [PubMed: 25957683]

Dawson AG. Oxidation of cytosolic NADH formed during aerobic metabolism in mammalian cells. Trends in Biochemical Sciences. 1979; 4:171–176.

de Brito OM, Scorrano L. Mitofusin 2 tethers endoplasmic reticulum to mitochondria. Nature. 2008; 456:605–610. [PubMed: 19052620]

Deberardinis RJ, Lum JJ, Thompson CB. Phosphatidylinositol 3-kinase-dependent modulation of carnitine palmitoyltransferase 1A expression regulates lipid metabolism during hematopoietic cell growth. J Biol Chem. 2006; 281:37372–37380. [PubMed: 17030509]

Frank M, Duvezin-Caubet S, Koob S, Occhipinti A, Jagasia R, Petcherski A, Ruonala MO, Priault M, Salin B, Reichert AS. Mitophagy is triggered by mild oxidative stress in a mitochondrial fission dependent manner. Biochim Biophys Acta. 2012; 1823:2297–2310. [PubMed: 22917578]

Frezza C, Cipolat S, Martins de Brito O, Micaroni M, Beznoussenko GV, Rudka T, Bartoli D, Polishuck RS, Danial NN, De Strooper B, Scorrano L. OPA1 controls apoptotic cristae remodeling independently from mitochondrial fusion. Cell. 2006; 126:177–189. [PubMed: 16839885]

Friedman JR, Nunnari J. Mitochondrial form and function. Nature. 2014; 505:335–343. [PubMed: 24429632]

Gomes LC, Di Benedetto G, Scorrano L. During autophagy mitochondria elongate, are spared from degradation and sustain cell viability. Nat Cell Biol. 2011; 13:589–598. [PubMed: 21478857]

Houtkooper RH, Pirinen E, Auwerx J. Sirtuins as regulators of metabolism and healthspan. Nat Rev Mol Cell Biol. 2012; 13:225–238. [PubMed: 22395773]

Huang SC, Everts B, Ivanova Y, O'Sullivan D, Nascimento M, Smith AM, Beatty W, Love-Gregory L, Lam WY, O'Neill CM, Yan C, Du H, Abumrad NA, Urban JF Jr, Artyomov MN, Pearce EL, Pearce EJ. Cell-intrinsic lysosomal lipolysis is essential for alternative activation of macrophages. Nat Immunol. 2014; 15:846–855. [PubMed: 25086775]

Kaech SM, Tan JT, Wherry EJ, Konieczny BT, Surh CD, Ahmed R. Selective expression of the interleukin 7 receptor identifies effector CD8 T cells that give rise to long-lived memory cells. Nat Immunol. 2003; 4:1191–1198. [PubMed: 14625547]

Krawczyk CM, Holowka T, Sun J, Blagih J, Amiel E, DeBerardinis RJ, Cross JR, Jung E, Thompson CB, Jones RG, Pearce EJ. Toll-like receptor-induced changes in glycolytic metabolism regulate dendritic cell activation. Blood. 2010; 115:4742–4749. [PubMed: 20351312]

Liesa M, Shirihai OS. Mitochondrial dynamics in the regulation of nutrient utilization and energy expenditure. Cell Metab. 2013; 17:491–506. [PubMed: 23562075]

MacIver NJ, Michalek RD, Rathmell JC. Metabolic regulation of T lymphocytes. Annu Rev Immunol. 2013; 31:259–283. [PubMed: 23298210]

Marsboom G, Toth PT, Ryan JJ, Hong Z, Wu X, Fang YH, Thenappan T, Piao L, Zhang HJ, Pogoriler J, Chen Y, Morrow E, Weir EK, Rehman J, Archer SL. Dynamin-related protein 1-mediated mitochondrial mitotic fission permits hyperproliferation of vascular smooth muscle cells and offers a novel therapeutic target in pulmonary hypertension. Circ Res. 2012; 110:1484–1497. [PubMed: 22511751]

Maus MV, Fraietta JA, Levine BL, Kalos M, Zhao Y, June CH. Adoptive immunotherapy for cancer or viruses. Annu Rev Immunol. 2014; 32:189–225. [PubMed: 24423116]

Mishra P, Carelli V, Manfredi G, Chan DC. Proteolytic cleavage of Opa1 stimulates mitochondrial inner membrane fusion and couples fusion to oxidative phosphorylation. Cell Metab. 2014; 19:630–641. [PubMed: 24703695]

Mishra P, Chan DC. Metabolic regulation of mitochondrial dynamics. J Cell Biol. 2016; 212:379–387. [PubMed: 26858267]

Nicholls DG. Spare respiratory capacity, oxidative stress and excitotoxicity. Biochem Soc Trans. 2009; 37:1385–1388. [PubMed: 19909281]

Nunnari J, Suomalainen A. Mitochondria: in sickness and in health. Cell. 2012; 148:1145–1159. [PubMed: 22424226]

O'Sullivan D, Pearce EL. Targeting T cell metabolism for therapy. Trends Immunol. 2015; 36:71–80. [PubMed: 25601541]

O'Sullivan D, van der Windt GJ, Huang SC, Curtis JD, Chang CH, Buck MD, Qiu J, Smith AM, Lam WY, DiPlato LM, Hsu FF, Birnbaum MJ, Pearce EJ, Pearce EL. Memory CD8(+) T cells use cell-intrinsic lipolysis to support the metabolic programming necessary for development. Immunity. 2014; 41:75–88. [PubMed: 25001241]

Patten DA, Wong J, Khacho M, Soubannier V, Mailloux RJ, Pilon-Larose K, MacLaurin JG, Park DS, McBride HM, Trinkle-Mulcahy L, Harper ME, Germain M, Slack RS. OPA1-dependent cristae modulation is essential for cellular adaptation to metabolic demand. EMBO J. 2014; 33:2676–2691. [PubMed: 25298396]

Pearce EL, Poffenberger MC, Chang CH, Jones RG. Fueling immunity: insights into metabolism and lymphocyte function. Science. 2013; 342:1242454. [PubMed: 24115444]

Pearce EL, Walsh MC, Cejas PJ, Harms GM, Shen H, Wang LS, Jones RG, Choi Y. Enhancing CD8 T-cell memory by modulating fatty acid metabolism. Nature. 2009; 460:103–107. [PubMed: 19494812]

Rambold AS, Cohen S, Lippincott-Schwartz J. Fatty acid trafficking in starved cells: regulation by lipid droplet lipolysis, autophagy, and mitochondrial fusion dynamics. Dev Cell. 2015; 32:678–692. [PubMed: 25752962]

Rambold AS, Kostelecky B, Elia N, Lippincott-Schwartz J. Tubular network formation protects mitochondria from autophagosomal degradation during nutrient starvation. Proc Natl Acad Sci U S A. 2011; 108:10190–10195. [PubMed: 21646527]

Restifo NP, Dudley ME, Rosenberg SA. Adoptive immunotherapy for cancer: harnessing the T cell response. Nat Rev Immunol. 2012; 12:269–281. [PubMed: 22437939]

Roth D, Krammer PH, Gulow K. Dynamin related protein 1-dependent mitochondrial fission regulates oxidative signalling in T cells. FEBS Lett. 2014; 588:1749–1754. [PubMed: 24681098]

Samant SA, Zhang HJ, Hong Z, Pillai VB, Sundaresan NR, Wolfgeher D, Archer SL, Chan DC, Gupta MP. SIRT3 deacetylates and activates OPA1 to regulate mitochondrial dynamics during stress. Mol Cell Biol. 2014; 34:807–819. [PubMed: 24344202]

Santel A, Frank S, Gaume B, Herrler M, Youle RJ, Fuller MT. Mitofusin-1 protein is a generally expressed mediator of mitochondrial fusion in mammalian cells. J Cell Sci. 2003; 116:2763–2774. [PubMed: 12759376]

Schluns KS, Williams K, Ma A, Zheng XX, Lefrancois L. Cutting edge: requirement for IL-15 in the generation of primary and memory antigen-specific CD8 T cells. J Immunol. 2002; 168:4827–4831. [PubMed: 11994430]

Sebastian D, Hernandez-Alvarez MI, Segales J, Sorianello E, Munoz JP, Sala D, Waget A, Liesa M, Paz JC, Gopalacharyulu P, Oresic M, Pich S, Burcelin R, Palacin M, Zorzano A. Mitofusin 2 (Mfn2) links mitochondrial and endoplasmic reticulum function with insulin signaling and is essential for normal glucose homeostasis. Proc Natl Acad Sci U S A. 2012; 109:5523–5528. [PubMed: 22427360]

Sena LA, Li S, Jairaman A, Prakriya M, Ezponda T, Hildeman DA, Wang CR, Schumacker PT, Licht JD, Perlman H, Bryce PJ, Chandel NS. Mitochondria are required for antigen-specific T cell activation through reactive oxygen species signaling. Immunity. 2013; 38:225–236. [PubMed: 23415911]

Serasinghe MN, Wieder SY, Renault TT, Elkholi R, Asciolla JJ, Yao JL, Jabado O, Hoehn K, Kageyama Y, Sesaki H, Chipuk JE. Mitochondrial division is requisite to RAS-induced transformation and targeted by oncogenic MAPK pathway inhibitors. Mol Cell. 2015; 57:521–536. [PubMed: 25658204]

Smith-Garvin JE, Koretzky GA, Jordan MS. T cell activation. Annu Rev Immunol. 2009; 27:591–619. [PubMed: 19132916]

Taguchi N, Ishihara N, Jofuku A, Oka T, Mihara K. Mitotic phosphorylation of dynamin-related GTPase Drp1 participates in mitochondrial fission. J Biol Chem. 2007; 282:11521–1159. [PubMed: 17301055]

Toyama EQ, Herzig S, Courchet J, Lewis TL Jr, Loson OC, Hellberg K, Young NP, Chen H, Polleux F, Chan DC, Shaw RJ. Metabolism. AMP-activated protein kinase mediates mitochondrial fission in response to energy stress. Science. 2016; 351:275–281. [PubMed: 26816379]

van der Windt GJ, Everts B, Chang CH, Curtis JD, Freitas TC, Amiel E, Pearce EJ, Pearce EL. Mitochondrial respiratory capacity is a critical regulator of CD8+ T cell memory development. Immunity. 2012; 36:68–78. [PubMed: 22206904]

van der Windt GJ, O'Sullivan D, Everts B, Huang SC, Buck MD, Curtis JD, Chang CH, Smith AM, Ai T, Faubert B, Jones RG, Pearce EJ, Pearce EL. CD8 memory T cells have a bioenergetic advantage that underlies their rapid recall ability. Proc Natl Acad Sci U S A. 2013; 110:14336–14341. [PubMed: 23940348]

Vander Heiden MG, Cantley LC, Thompson CB. Understanding the Warburg effect: the metabolic requirements of cell proliferation. Science. 2009; 324:1029–1033. [PubMed: 19460998]

Wai T, Langer T. Mitochondrial Dynamics and Metabolic Regulation. Trends Endocrinol Metab. 2016; 27:105–117. [PubMed: 26754340]

Wang D, Wang J, Bonamy GM, Meeusen S, Brusch RG, Turk C, Yang P, Schultz PG. A small molecule promotes mitochondrial fusion in mammalian cells. Angew Chem Int Ed Engl. 2012; 51:9302–9305. [PubMed: 22907892]

Wang L, Ishihara T, Ibayashi Y, Tatsushima K, Setoyama D, Hanada Y, Takeichi Y, Sakamoto S, Yokota S, Mihara K, Kang D, Ishihara N, Takayanagi R, Nomura M. Disruption of mitochondrial fission in the liver protects mice from diet-induced obesity and metabolic deterioration. Diabetologia. 2015; 58:2371–2380. [PubMed: 26233250]

Wang R, Green DR. Metabolic checkpoints in activated T cells. Nat Immunol. 2012; 13:907–915. [PubMed: 22990888]

Williams MA, Bevan MJ. Effector and memory CTL differentiation. Annu Rev Immunol. 2007; 25:171–192. [PubMed: 17129182]

Youle RJ, Karbowski M. Mitochondrial fission in apoptosis. Nat Rev Mol Cell Biol. 2005; 6:657–663. [PubMed: 16025099]

Yu T, Robotham JL, Yoon Y. Increased production of reactive oxygen species in hyperglycemic conditions requires dynamic change of mitochondrial morphology. Proc Natl Acad Sci U S A. 2006; 103:2653–2658. [PubMed: 16477035]

Zhang Z, Wakabayashi N, Wakabayashi J, Tamura Y, Song WJ, Sereda S, Clerc P, Polster BM, Aja SM, Pletnikov MV, Kensler TW, Shirihai OS, Iijima M, Hussain MA, Sesaki H. The dynamin-related GTPase Opa1 is required for glucose-stimulated ATP production in pancreatic beta cells. Mol Biol Cell. 2011; 22:2235–2245. [PubMed: 21551073]

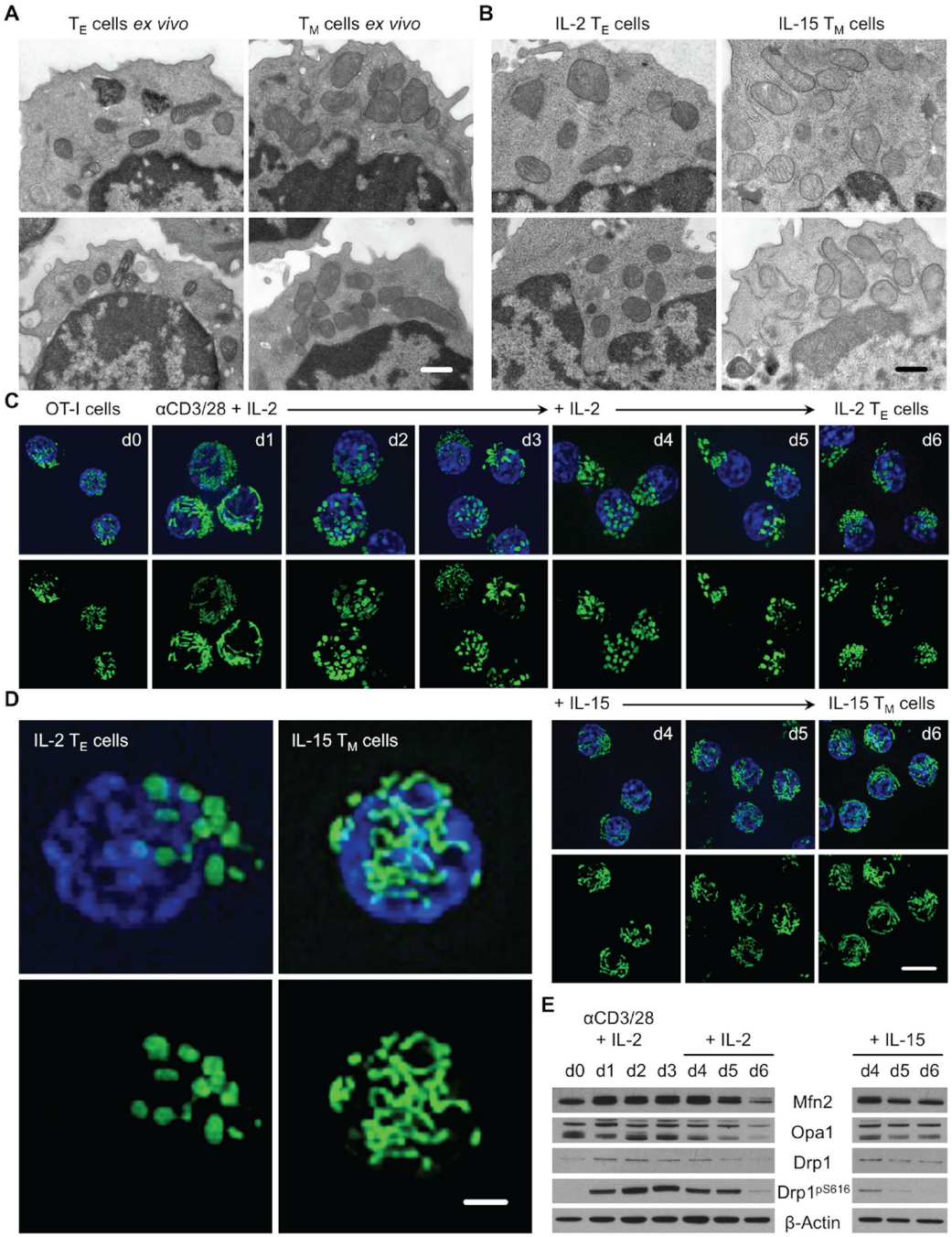

Figure 1. Effector and memory T cells possess distinct mitochondrial morphologies

(**A**) Effector (T_E, CD44^{hi} CD62L^{lo}, 7 days post infection) and memory T (T_M, CD44^{hi} CD62L^{hi}, 21 days post infection) cells sorted from C57BL/6 mice infected i.p. with 10^7 CFU LmOVA and (**B**) IL-2 T_E and IL-15 T_M cells generated from differential culture of OT-I cells activated with OVA peptide and IL-2 using IL-2 or IL-15 analyzed by EM, scale bar = 0.5 μm. (**C–D**) Mitochondrial morphology in live OT-I PhAM cells before and after αCD3/CD28 activation and differential cytokine culture by spinning disk confocal microscopy. Mitochondria are green (GFP) and nuclei are blue (Hoechst), (**C**) scale bar = 5 μm, (**D**) scale

bar = 1 μm. (**E**) Immunoblot analysis of cell protein extracts from (**C**), probed for Mfn2, Opa1, Drp1, phosphorylated Drp1 at Ser616 ($Drp1^{pS616}$), and β-actin. (**A–E**) Representative of 2 experiments. **See also** Figure S1.

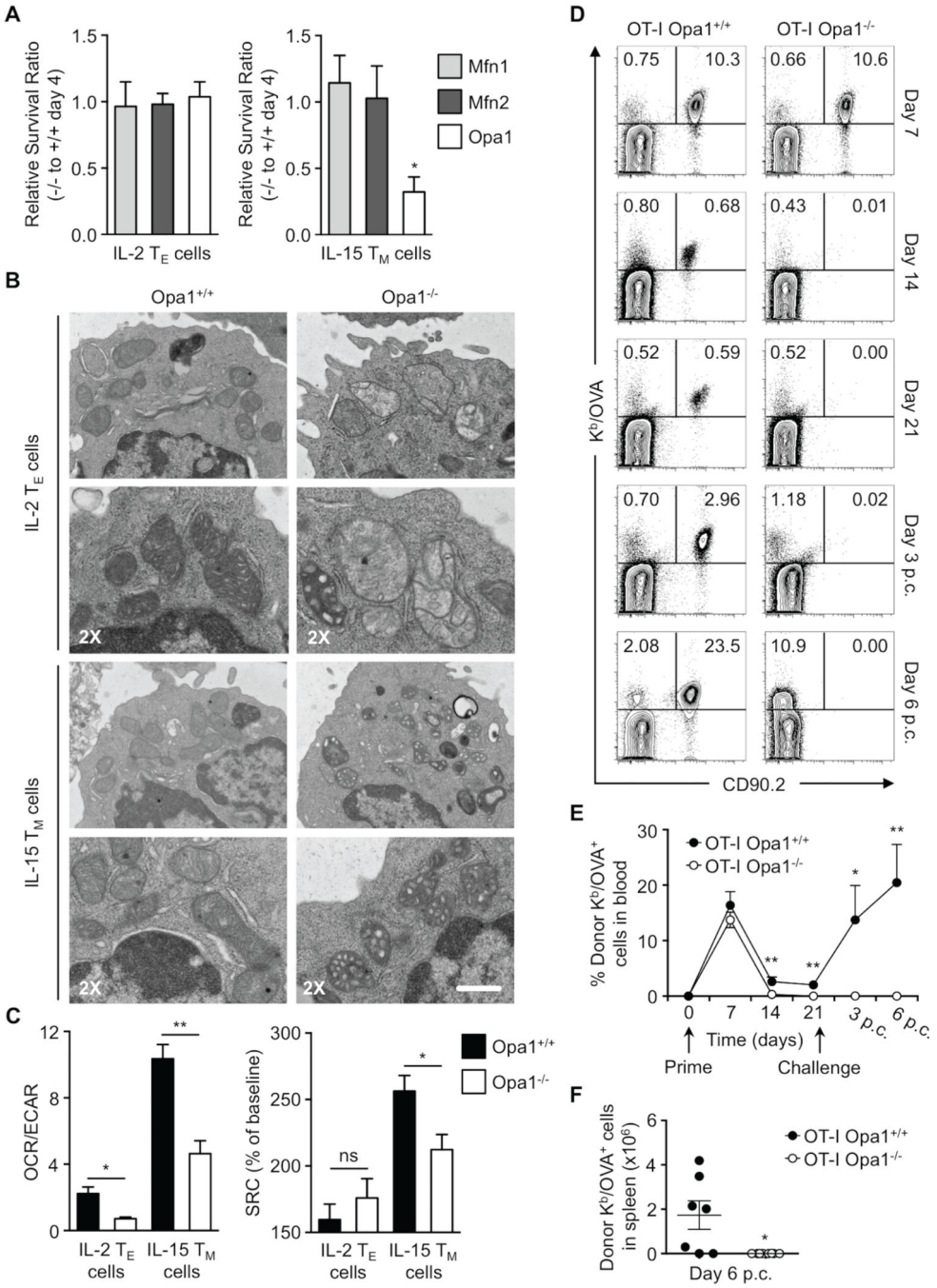

Figure 2. Memory T cell development and survival, unlike effectors, requires mitochondrial fusion

(**A**) Relative *in vitro* survival ratios of Mfn1, Mfn2, or Opa1 deficient (CD4 Cre^{+}, −/−) to wild-type (CD4 Cre^{-}, +/+) OT-I IL-2 T_E and IL-15 T_M cells (*p=0.0465). Data normalized from 2–3 independent experiments shown as mean ± SEM. (**B**) Mitochondrial morphology of OT-I Opa1 wild-type and $Opa1^{-/-}$ IL-2 T_E and IL-15 T_M cells analyzed by EM (scale bar = 0.5 μm, represents one experiment) and (**C**) Seahorse EFA. (Left) bar graph represents ratios of O_2 consumption rates (OCR, indicator of OXPHOS) to extracellular acidification

rates (ECAR, indicator of aerobic glycolysis) at baseline and (right) spare respiratory capacity (SRC) (% max OCR after FCCP injection of baseline OCR) of indicated cells (*p<0.03, **p=0.0079). Data from 3 experiments shown as mean ± SEM. (**D–F**) 10^4 OT-I $Opa1^{+/+}$ or $Opa1^{-/-}$ T cells were transferred i.v. into C57BL/6 CD90.1 mice infected i.v. with 10^7 CFU LmOVA. Blood analyzed by flow cytometry at indicated times post infection. After 21 days, mice were challenged i.v. with 5×10^7 CFU LmOVA and blood analyzed post challenge (p.c.). (**D**) % Donor K^b/OVA^+ $CD90.2^+$ cells shown in representative flow plots and (**E**) line graph with mean ± SEM (*p=0.0238, **p<0.005). (**F**) Number of donor K^b/OVA^+ cells from spleens of infected mice shown with mean ± SEM (*p=0.0126). (**D–F**) Representative of 2 experiments (n=9–11/ group). **See also** Figure S2.

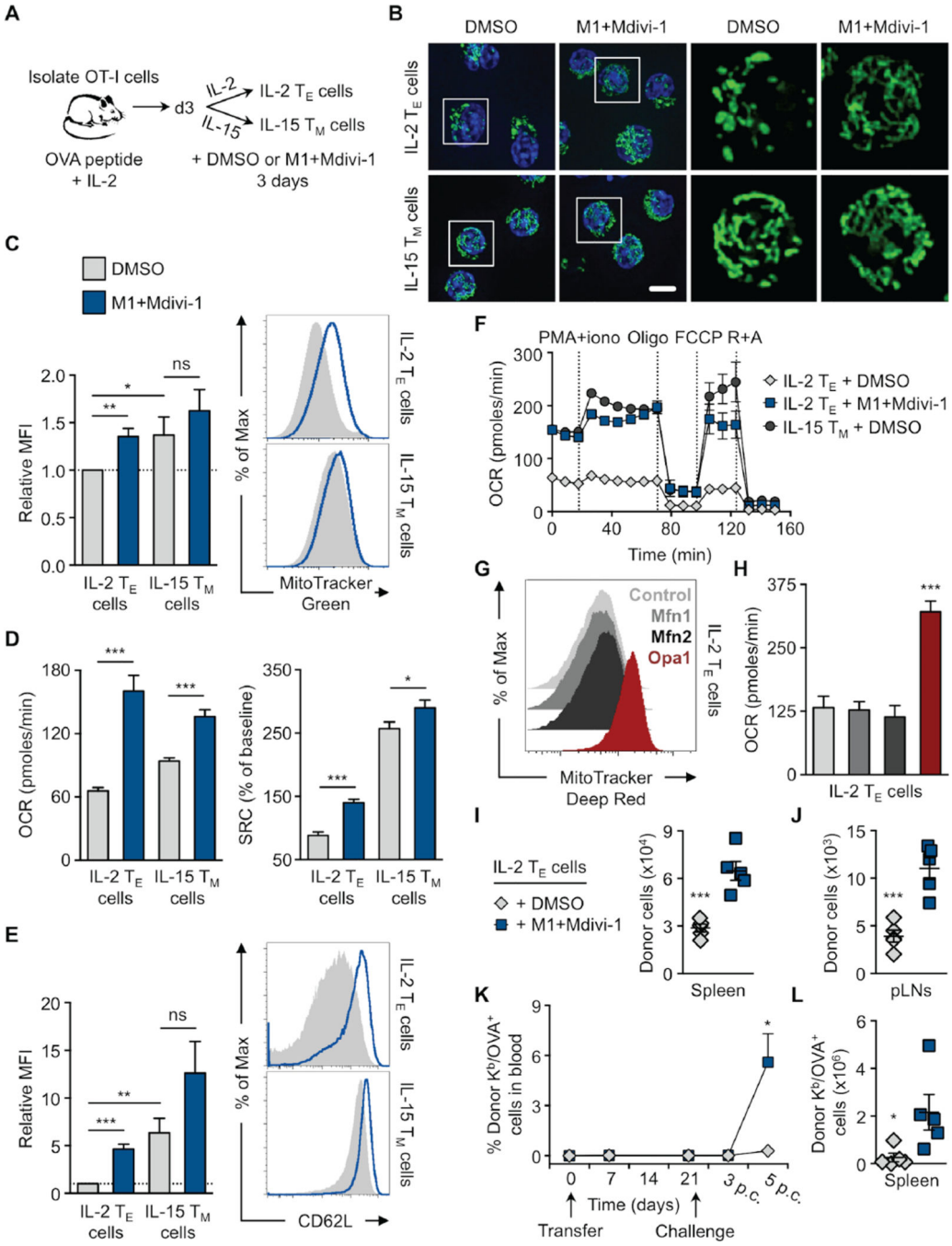

Figure 3. Enhancing mitochondrial fusion promotes the generation of memory-like T cells

(**A–F**, **I–L**) OVA peptide and IL-2 activated OT-I cells differentiated into IL-2 T_E or IL-15 T_M cells for 3 days in the presence of DMSO or 20 μM fusion promoter M1 and 10 μM fission inhibitor Mdivi-1 (M1+Mdivi-1) as shown (**A**) pictorially. (**B**) Representative spinning disk confocal images from 3 experiments of live cells from OT-I PhAM mice. Mitochondria are green (GFP) and nuclei are blue (Hoechst), scale bar = 5 μm. (**C**) Cells stained with MitoTracker Green and analyzed by flow cytometry. Relative MFI (left) from 6 experiments (*p=0.0394, **p=0.0019) with representative histograms (right). (**D**) Baseline

OCR and SRC from 3–4 experiments (*p=0.0485, ***p<0.0001) and (**E**) CD62L expression analyzed by flow cytometry of indicated cells. Relative MFI (left) from 7 experiments (*p=0.0325, **p=0.0019, ***p<0.0001) with representative histograms (right). (**F**) OCR of indicated cells at baseline and in response to PMA and ionomycin stimulation (PMA+iono), oligomycin (Oligo), FCCP, and rotenone plus antimycin A (R+A). Represents 2 experiments. (**C–F**) Shown as mean ± SEM. (**G–H**) OT-I cells were transduced with either empty (Control), Mfn1, Mfn2, or Opa1 expression vectors, sorted, and cultured to generate IL-2 T_E cells. (**G**) Representative histograms of MitoTracker Deep Red staining from 4 experiments and (**H**) basal OCR from 2 experiments of transduced cells. (**I–L**) 1–2×10^6 IL-2 T_E cells cultured with DMSO (gray diamonds) or M1+Mdivi-1 (blue squares) were transferred into congenic C57BL/6 recipient mice. Cell counts of donor cells recovered 2 days later from the (**I**) spleen (***p=0.005) and (**J**) peripheral lymph nodes (pLNs, ***p=0.0006). Dots are individual mice. (**K**) Blood from recipient mice analyzed for % donor K^b/OVA^+ cells post transfer and challenge with 10^7 CFU LmOVA by flow cytometry (*p=0.0150, n=5/group). (**L**) Donor K^b/OVA^+ cells recovered from recipient spleens 6 days p.c. (*p=0.0383). Dots are individual mice (**I–L**) Represents 2 experiments shown with mean ± SEM. **See also** Figure S3.

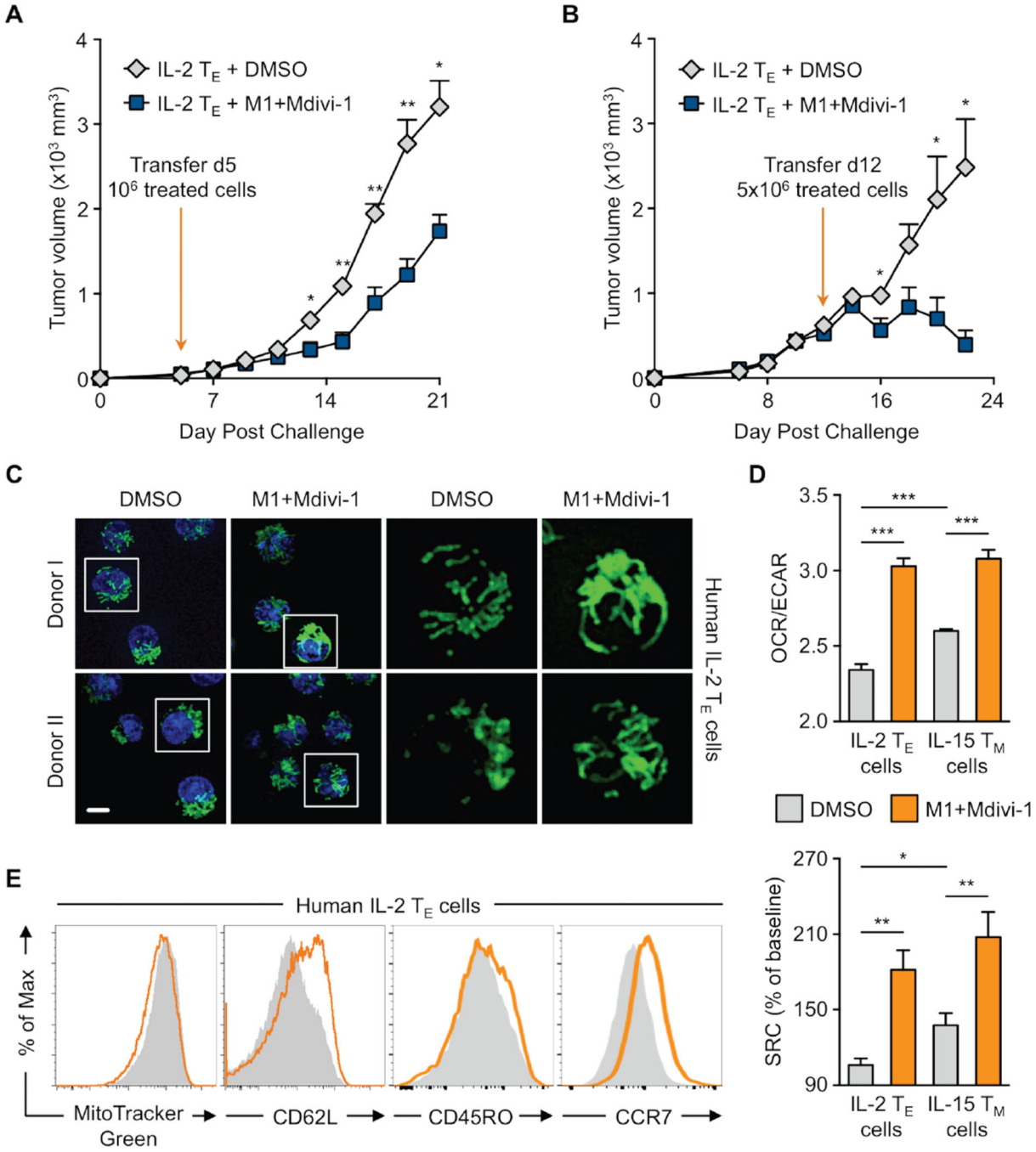

Figure 4. Mitochondrial fusion improves adoptive cellular immunotherapy against tumors

(**A–B**) C57BL/6 mice inoculated s.c. with 10^6 EL4-OVA cells. (**A**) After 5 or (**B**) 12 days, 10^6 or 5×10^6 OT-I IL-2 T_E cells cultured with DMSO or M1+Mdivi-1 were transferred i.v. into recipients and tumor growth assessed. Represents 2 experiments shown as mean ± SEM (n=5/group, *p<0.05, **p<0.005). (**C-E**) Human $CD8^+$ PBMCs activated with αCD3/CD28 + IL-2 to generate IL-2 T_E cells. (**C**) Confocal images of indicated cells where mitochondria are green (MitoTracker) and nuclei are blue (Hoechst). Representative images from 2 of 4 biological donors, scale bar = 5 μm. (**D**) OCR/ECAR ratios and SRC of indicated cells from

2 separate donors shown as mean ± SEM (*p=0.0303, **p<0.005, ***p<0.0001). (**E**) MitoTracker Green staining and CD62L, CD45RO, and CCR7 expression analyzed by flow cytometry shown with representative histograms from 4–6 biological replicates. **See also** Figure S4.

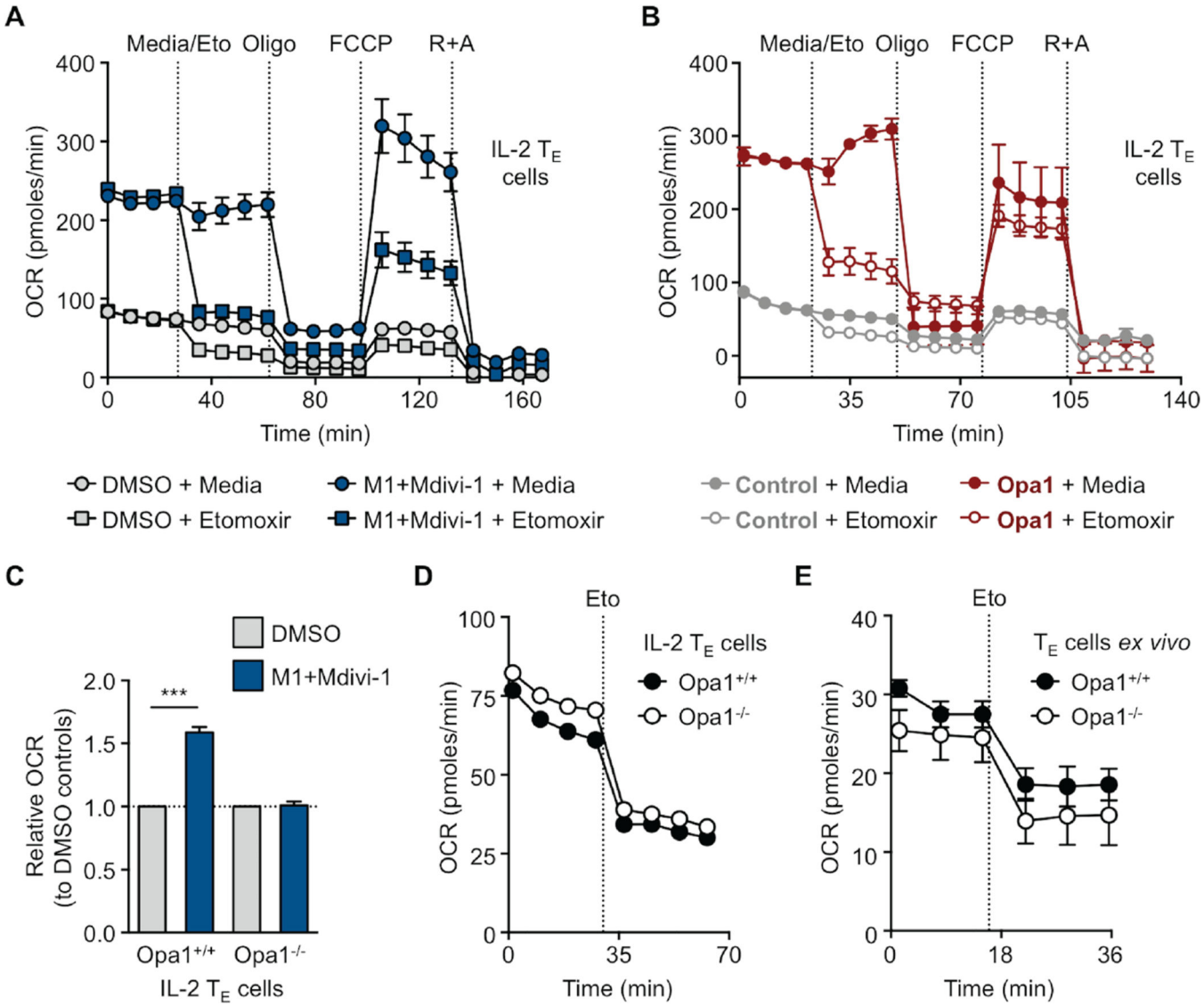

Figure 5. Fusion promotes memory T cell metabolism, but Opa1 is not required for FAO

(**A–E**) OCR measured at baseline and in response to media, etomoxir (Eto) and other drugs as indicated of (**A**) IL-2 T_E cells cultured in DMSO or M1+Mdivi-1, (**B**) control or Opa1 transduced IL-2 T_E cells, (**C**) $Opa1^{+/+}$ and $Opa1^{-/-}$ IL-2 T_E cells cultured in DMSO or M1+Mdivi-1 (**D**) or without drugs, and (**E**) *ex vivo* donor OT-I $Opa1^{+/+}$ and $Opa1^{-/-}$ day 7 T_E cells derived from LmOVA infection. (**A-E**) Representative of 2 experiments shown as mean ± SEM (***p<0.0001). **See also** Figure S5.

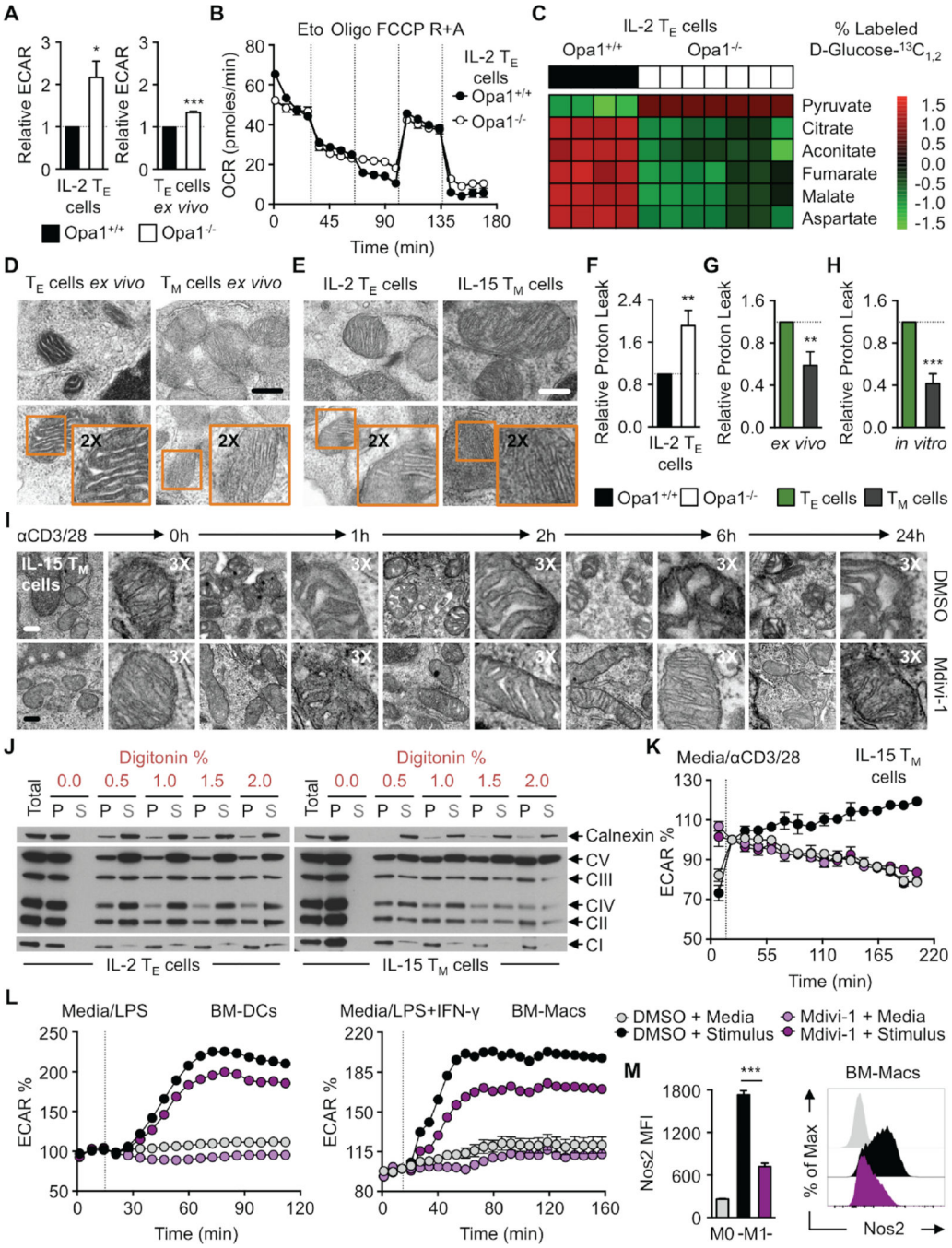

Figure 6. Mitochondrial cristae remodeling signals metabolic pathway engagement

(**A**) Basal ECAR of OT-I Opa1$^{+/+}$ and Opa1$^{-/-}$ IL-2 T_E cells (left) and day 7 T_E cells isolated *ex vivo* after adoptive transfer from LmOVA infection (right). Data combined from 2–3 experiments (*p=0.0412, ***p<0.0001). (**B**) OCR at baseline and with indicated drugs, representative of 2 experiments shown as mean ± SEM and (**C**) D-Glucose-$^{13}C_{1,2}$ trace analysis of OT-I Opa1$^{+/+}$ and Opa1$^{-/-}$ IL-2 T_E cells. Each lane represents separate mice with a technical replicate. (**D**) EM analysis of mitochondrial cristae from T_E and T_M cells isolated after LmOVA infection and (**E**) *in* vitro cultured IL-2 T_E and T_M cells. Representative of 2

experiments, scale bar = 0.25 μm. Relative proton leak (ΔOCR after oligomycin and subsequent injection of rotenone plus antimycin A) of (**F**) $Opa1^{+/+}$ and $Opa1^{-/-}$ IL-2 T_E, (**G**) infection elicited T_E and T_M, and (**H**) IL-2 T_E and IL-15 T_M cells. (**F–H**) Combined from 2–4 experiments shown as mean ± SEM (p**<0.005, ***p<0.0001). (**I**) EM analysis of IL-15 T_M cell-mitochondrial cristae before and after αCD3/CD28 bead stimulation over hours. Scale bar = 0.2 μm, represents one experiment. (**J**) Immunoblot analysis of Calnexin and ETC complexes (CI-NDUFB8, CII-SDHB, CIII-UQCRC2, CIV-MTC01, CV-ATP5A). Equivalent numbers of IL-2 T_E and IL-15 T_M cells lysed in native lysis buffer followed by digitonin solubilization of intracellular membranes with pellet (P) and solubilized supernatant (S) fractions resolved on a denaturing gel, representative of 2 experiments. (**K**) IL-15 T_M cell, (**L**) BM-DCs and BM-Macs % ECAR measured at baseline and after media, αCD3/CD28 bead, LPS, or LPS+IFN-γ injection as indicated. Data baselined prior to or right after injection with stimuli. (**M**) BM-Macs stained for intracellular Nos2 protein by flow cytometry with MFI values (left) and representative histogram (right). (**K–M**) Shown as mean ± SEM and represent 2–3 experiments (***p<0.0001). **See also** Figure S6.